NASA Contractor Report 181921
ICASE Report No. 89–68

ICASE

CONVECTION OF A PATTERN OF VORTICITY THROUGH A REACTING SHOCK WAVE

T. L. Jackson
A. K. Kapila
M. Y. Hussaini

Contract Nos. NAS1–18107, NAS1–18605
September 1989

Institute for Computer Applications in Science and Engineering
NASA Langley Research Center
Hampton, Virginia 23665–5225

Operated by the Universities Space Research Association

(NASA-CR-181921) CONVECTION OF A PATTERN OF VORTICITY THROUGH A REACTING SHOCK WAVE Final Report (ICASE) 33 p CSCL 12A

N90-10576

Unclas
G3/59 0235050

National Aeronautics and
Space Administration

Langley Research Center
Hampton, Virginia 23665-5225

CONVECTION OF A PATTERN OF VORTICITY THROUGH A REACTING SHOCK WAVE

T. L. Jackson
Department of Mathematics and Statistics
Old Dominion University
Norfolk, Virginia 23529

A. K. Kapila
Department of Mathematical Sciences
Rensselaer Polytechnic Institute
Troy, New York 12180-3590

M. Y. Hussaini
Institute for Computer Applications in Science and Engineering
NASA Langley Research Center
Hampton, Virginia 23665

ABSTRACT

The passage of a weak vorticity disturbance through a reactive shock wave, or detonation, is examined by means of a linearized treatment. Of special interest is the effect of chemical heat release on the amplification of vorticity in particular, and on the disturbance pattern generated downstream of the detonation in general. It is found that the effect of exothermicity is to amplify the refracted waves. The manner in which the imposed disturbance alters the structure of the detonation itself is also discussed.

This work was supported by the National Aeronautics and Space Administration under NASA Contracts NAS1-18107 and NAS1-18605, while the authors were in residence at the Institute for Computer Applications in Science and Engineering, NASA Langley Research Center, Hampton, Virginia 23665. A.K.K. was also supported partially by the Army Research Office.

INTRODUCTION

When a pattern of vorticity in an otherwise uniform stream passes through a plane shock, it undergoes refraction and amplification, with the simultaneous generation of acoustic and entropy signals behind the shock. For small amplitudes of incident disturbance, a linearized analysis is possible, and has indeed been carried out by several authors; see, for example, Ribner [1], McKenzie and Westphal [2] and Anyiwo and Bushnell [3]. The predictions of the linear theory and departures therefrom have been examined by Zang, Hussaini and Bushnell [4] via two-dimensional numerical simulations.

The above studies have all been confined to chemically inert flows. With renewed interest in hypersonic vehicles, there has emerged a need for improved understanding of shock-turbulence interactions in reacting flows. This paper addresses a specific reactive-flow configuration, namely, a planar standing detonation wave (reacting shock wave). Such waves, provided they can be stabilized (still a matter under exploration), have been proposed as an alternative to the SCRAMJET concept in high-speed propulsion (O'Brien and Kobayashi [5]). Our aim is to examine the interactions of the detonation with a small-amplitude shear wave as the latter is convected through the detonation. This is accomplished by means of a linear analysis, which can be thought of as an extension of Ribner's [1] for an inert shock. Unlike Ribner, however, we are interested not only in the effect of the detonation on the disturbance, but also on the manner in which the shape and structure of the detonation are altered by the disturbance.

THE GOVERNING EQUATIONS

Figure 1 illustrates a stationary, planar, oblique detonation wave, into which flows an unburnt mixture of reactants from the left, with burnt products emerging on the right. The undisturbed flow is assumed to be uniform on either side, with the normal component of velocity supersonic ahead of the wave and subsonic behind. In the (x, y) coordinate frame the detonation shock is represented by $x = 0$, the $x-$axis being normal to the shock. (The analysis assumes that there are no variations in the $z-$direction.) The (ξ, η) coordinate frame is aligned with the downstream flow, and the (ξ', η') frame with the upstream flow.

Let us now suppose that a planar, steady, shear disturbance, whose amplitude is small and depends only on the cross-stream coordinate η', is superimposed on the incident stream (Figure 2). The intent is to compute the perturbed flowfield behind the detonation and the perturbation of the detonation structure.

It is convenient to nondimensionalize the system. Accordingly, the pressure, temperature and density of the gas, and the mass fraction of the reactant in the mixture, are referred to their respective values in the unreacted, unperturbed gas ahead of the detonation. Velocities are referred to the frozen sound speed in the unperturbed gas, and lengths to the characteristic wavelength of the disturbance. Then, the basic equations expressed in the downstream coordinates (ξ, η) are

$$(\rho u)_\xi + (\rho v)_\eta = 0, \tag{1a}$$

$$\rho(uu_\xi + vu_\eta) + (1/\gamma)p_\xi = 0, \tag{1b}$$

$$\rho(uv_\xi + vv_\eta) + (1/\gamma)p_\eta = 0, \tag{1c}$$

$$\rho(uT_\xi + vT_\eta) - \frac{\gamma - 1}{\gamma}(up_\xi + vp_\eta) = \alpha\rho\Lambda, \tag{1d}$$

$$p = \rho T, \tag{1e}$$

and

$$uY_\xi + vY_\eta = -\Lambda, \tag{1f}$$

where

$$\Lambda = \frac{AL_0}{\overline{c}} e^{-E/T}. \tag{1g}$$

Here, (u, v) is the gas velocity, Y the reactant mass fraction, and ρ, p and T the density, pressure and temperature respectively. A single irreversible reaction of type $A \rightarrow B$, governed by Arrhenius kinetics, has been postulated. (The details of the reaction scheme will only influence the effect of the disturbance on the detonation structure; the effect of the detonation on the disturbance depends only on the overall heat release.) The dimensionless parameters γ, E and α are, respectively, the ratio of specific heats, the activation energy and the heat release parameter. These are defined in terms of appropriate dimensional or reference quantities by the expressions

$$\gamma = C_p/C_v, \quad \alpha = \overline{QY}/C_p\overline{T}, \quad E = \overline{E}/R\overline{T},$$

where $\overline{Y}$ is the reactant mass fraction and $\overline{T}$ the temperature of the fresh mixture, while $\overline{Q}$ is the heat released when a unit mass of the reactant is consumed. The dimensional activation energy is denoted by $\overline{E}$, the gas constant by R and the specific heats at constant pressure and volume by C_p and C_v respectively. Finally, L_0 is the characteristic wave length of the disturbance, $\overline{c}$ the sound speed in the unburnt gas, and A the pre-exponential factor in the Arrhenius rate law.

Typically L_0 is much larger than the thickness of the detonation, so that on the scale of the disturbance, the detonation can be treated as a discontinuity in an inert flow. When

examining the effect of the detonation on the disturbance, therefore, equation (1f) can be replaced by

$$Y = 1 \text{ ahead of the detonation,} \qquad 0 \text{ behind the detonation.}$$

However, (1f) will need to be reinstated, and the entire equation set (1) rescaled with respect to the detonation thickness, when assessing the effect of the disturbance on the detonation structure.

EFFECT OF DETONATION ON DISTURBANCE

With the detonation treated as a discontinuity, the generalized Rankine-Hugoniot conditions yield the following expressions for the state of the gas behind it:

$$m = \frac{1+\gamma M^2}{(\gamma+1)M} - \frac{1}{(\gamma+1)}\left[\frac{(M^2-1)^2}{M^2} - 2(\gamma+1)\alpha\right]^{1/2}, \tag{2a}$$

$$\rho = M/m, \tag{2b}$$

$$T = 1 + \alpha + \frac{(\gamma-1)}{2}(M^2 - m^2), \tag{2c}$$

$$p = \rho T = \frac{M}{m}\left[1 + \alpha + \frac{(\gamma-1)}{2}(M^2 - m^2)\right], \tag{2d}$$

$$w = W \text{ or equivalently, } m\tan\varphi = M\tan\theta. \tag{2e}$$

Here, m is the normal velocity and w the tangential velocity behind the discontinuity, while M and W are the corresponding quantities ahead. Observe that M is also the normal Mach number in the unburnt region. The minimum value M_{CJ} of M, corresponding to a Chapman-Jouguet wave, is given by

$$M_{CJ} = \left[1 + (\gamma+1)\alpha + \left[\{1+(\gamma+1)\alpha\}^2 - 1\right]^{1/2}\right]^{1/2}. \tag{3}$$

A graph of M_{CJ} against α is shown in Figure 3.

Let the perturbed upstream flow be characterized by

$$U = U_0 + U_1, \qquad U_1 << U_0, \tag{4a}$$

and correspondingly (see Figure 4),

$$\theta = \theta_0 + \theta_1, \quad M = M_0 + M_1, \quad W = W_0 + W_1, \tag{4b}$$

while all other state variables upstream remain unchanged. (The precise form of U_1 will be specified later.) It is now a simple matter to linearize the jump-relations (2) to obtain the following expressions for the disturbances immediately behind the detonation front (identified by the suffix f):

$$u_{1f}/m_0 = -d\cos\varphi_0[(U_1/U_0) - (\theta_1/r)\tan\varphi_0] + \sin\varphi_0[\theta_1 r + (U_1/U_0)\tan\varphi_0], \tag{5a}$$

$$v_{1f}/m_0 = d\sin\varphi_0[(U_1/U_0) - (\theta_1/r)\tan\varphi_0] - \theta_1\sec\varphi_0 + \cos\varphi_0[\theta_1 r + (U_1/U_0)\tan\varphi_0], \tag{5b}$$

$$p_{1f} = \gamma M_0^2[2 - (1-d)/r][(U_1/U_0) - (\theta_1/r)\tan\varphi_0], \tag{5c}$$

$$T_{1f} = (\gamma-1)M_0^2(1 + d/r^2)[(U_1/U_0) - (\theta_1/r)\tan\varphi_0]. \tag{5d}$$

The constant r is simply the ratio of the normal speeds across the detonation,

$$r = M_0/m_0, \tag{6}$$

while d is defined by

$$d = \frac{1}{(\gamma+1)M_0 m_0}\left[1 - \gamma M_0^2 + \frac{M_0^4 - 1}{\{(M_0^2-1)^2 - 2(\gamma+1)\alpha M_0^2\}^{1/2}}\right]. \tag{7}$$

The expressions (5) act as boundary conditions for the perturbed flow downstream of the detonation. The governing equations for this flow are simply the Euler equations (1a-e). Upon linearization about the basic downstream state these reduce to

$$(1-\mu^2)\psi_{\xi\xi} + \psi_{\eta\eta} = -\Omega_1(\eta). \tag{8}$$

where ψ is the perturbation stream function, μ the Mach number of the undisturbed downstream flow, defined by

$$\mu = (u_0^2/T_0)^{1/2}, \tag{9}$$

and Ω_1 the vorticity behind the wave. It can be shown that Ω_1 depends on the cross-stream coordinate η alone, and can therefore be evaluated at the location of the undisturbed front, again identified by the suffix f, i.e.,

$$\Omega_1 = -\left[\frac{1}{\rho_0 u_0 \gamma}p_{1\eta} + u_{1\eta}\right]_f. \tag{10}$$

Once ψ is known, the velocity components are given by the expressions

$$u_1 = \psi_\eta, \qquad v_1 = -(1-\mu^2)\psi_\xi, \tag{11}$$

while pressure, temperature and density can be found from

$$p_1 = p_{1f} + \gamma\rho_0 u_0(u_{1f} - u_1), \tag{12a}$$

$$T_1 = T_{1f} + \frac{(\gamma-1)}{\gamma\rho_0}(p_1 - p_{1f}), \tag{12b}$$

$$\rho_1 = (1/T_0)(p_1 - \rho_0 T_1). \tag{12c}$$

Now, depending upon the downstream Mach number μ, equation (8) is either elliptic ($\mu < 1$) or hyperbolic ($\mu > 1$). In turn, μ is an increasing function of the inclination θ_0 of the incident stream for a given upstream normal Mach number M_0. In fact, there exists a critical value θ_c of θ_0, given by

$$\tan\theta_c = \left[\{2(1+\alpha) + (\gamma-1)M_0^2 - (\gamma+1)m_0^2\}/(2M_0^2)\right]^{1/2}, \tag{13}$$

such that $\mu > 1$ for $\theta > \theta_c$ and $\mu < 1$ for $\theta < \theta_c$. Figure 5 shows a plot of θ_c as a function of the upstream normal Mach number M_0 (more specifically, M_0/M_{CJ}) for various values of the heat-release parameter α. Observe that for a $CJ-$detonation, the downstream flow is supersonic for all $\theta_0 > 0$.

Thus far, the formulation has been quite independent of the functional form of the incident disturbance. Following Ribner [1], let us take a sinusoidal perturbation, i.e.,

$$U_1 = \epsilon U_0 \cos k'\eta', \tag{14}$$

where ϵ characterizes the perturbation amplitude and k' is the incident wave number. The downstream wave number k, given by

$$k'\cos\theta_0 = k\cos\varphi_0, \tag{15}$$

must also satisfy the matching requirement

$$k'\eta' = k\eta \tag{16}$$

at the front. Therefore,

$$U_1 = \epsilon U_0 \cos k\eta \text{ at the front.} \tag{17}$$

The corresponding perturbation in the front inclination may be taken to be

$$\theta_1 = \epsilon(a\cos k\eta + b\sin k\eta), \tag{18}$$

where a and b are to be determined.

The problem now reduces to the following: using the prescriptions (17) and (18) in the boundary conditions $(5a, b)$, solve (8) for ψ. Then, u_1 and v_1 can be found from (11) and the remaining variables from (12) upon using the conditions (5). Only the results are given below since computational details are similar to those in Ribner [1]. (We have elected to display the velocity and pressure fields only; temperature and density follow from $(12b, c)$ in a straightforward manner.)

For $\mu < 1$ the solution is

$$(19a) \qquad \begin{aligned} u_1/(\epsilon U_0) = {} & S\cos[k_y(y - x\tan\varphi_0) + \delta_s] \\ & + P(x)\cos[k_y(y - x\tan\varphi_0') + \delta_p], \end{aligned}$$

$$(19b) \qquad v_1/(\epsilon U_0) = \beta P(x)\sin[k_y(y - x\tan\varphi_0') + \delta_p],$$

$$(19c) \qquad p_1/(\epsilon U_0) = -\gamma M_0 P(x)\sec\varphi_0\cos[k_y(y - x\tan\varphi_0') + \delta_p],$$

where

$$(20) \qquad \beta = (|1 - \mu^2|)^{1/2}, \qquad \beta_n^2 = 1 - \mu^2\cos^2\varphi_0,$$

$$(21) \qquad k_y = k\cos\theta_0,$$

and

$$(22a) \qquad P(x) = [1/(\beta r)](C_1^2 + C_2^2)^{1/2}\exp(-k_y\beta x/\beta_n^2)\cos\theta_0,$$

$$(22b) \qquad S = (A^2 + B^2)^{1/2}(1/r)\cos\theta_0,$$

$$(22c) \qquad \delta_s = \tan^{-1}(-B/A),$$

$$(22d) \qquad \delta_p = \tan^{-1}[(C_1\beta - C_2\tan\varphi_0)/(C_2\beta + C_1\tan\varphi_0)],$$

$$(22e) \qquad \varphi_0' = -\tan^{-1}[(\mu/\beta)^2\cos^2\varphi_0\tan\varphi_0].$$

The constants A, B, C_1 and C_2 appearing above have been defined in the Appendix, along with the constants a and b introduced in (18).

For $\mu > 1$,

$$u_1/(\epsilon U_0) = S\cos[k_y(y - x\tan\varphi_0)] + P\cos[k_y(y - x\tan\varphi_0')], \tag{23a}$$

$$v_1/(\epsilon U_0) = \beta P\cos[k_y(y - x\tan\varphi_0')], \tag{23b}$$

$$p_1/(\epsilon U_0) = -\gamma M_0 P\sec\varphi_0\cos[k_y(y - x\tan\varphi_0')], \tag{23c}$$

where

$$P = (C_1/r)(\cos\theta_0\sin\omega)/\cos\varphi_0', \tag{24a}$$

$$\omega = \cot^{-1}\beta_n, \tag{24b}$$

$$S = (A/r)\cos\theta_0, \tag{24c}$$

$$\varphi_0' = \varphi_0 - \omega. \tag{24d}$$

An examination of (19) and (23) reveals that the velocity field is made up of a shear component of amplitude S and a potential-flow component of amplitude P. The shear component is a plane wave which carries all the vorticity and propagates in the streamwise direction. The potential component, as Ribner [1] has pointed out, is acoustic in character and is the sole contributor to the pressure disturbance. It also travels as a wave, but in a direction inclined at an angle φ' to the normal, with amplitude remaining constant for the supersonic case and attenuating exponentially for the subsonic. The subsonic flow involves phase shifts δ_s and δ_p, while the supersonic flow does not.

The amplitude S and the phase shift δ_s are plotted in Figure 6(a,b), against the wave inclination θ_0, at $M_0/M_{CJ} = 1.5$ and for various values of the heat release α. The most dramatic effect occurs at the sonic point, $\theta = \theta_c$, where the amplitude increases sharply. Figure 6(c) displays the maximum amplitude as a function of α for four different values of the incident Mach number, and reveals that for α beyond 0.5, the graphs are essentially linear. In Figure 7(a,b,c) the corresponding graphs for P, the amplitude of the potential component (evaluated at the shock for subsonic flow), and the phase shift δ_p are shown. The behavior is similar to that in Figure 6, with one exception: whereas the maximum amplitude of the shear component increases with increase in M_0/M_{CJ} (Figure 6c), that of the potential component decreases (Figure 7c).

Because of the nonuniform pressure jump across the front, it develops ripples, and the resulting deflection of the front from the undisturbed position $x = 0$ (obtained by integrating the front-deflection angle θ_1) is found to be

$$\Delta_f = [\epsilon U_0/(k' M_0)](a^2 + b^2)^{1/2}\cos(k_y y + \delta_{\text{front}}), \tag{25}$$

where k' is the wavenumber of the incident disturbance and a, b (introduced in (18)) are defined in the Appendix. The quantities $(a^2 + b^2)^{1/2}$ and δ_{front} have been plotted in Figure 8(a,b) against the wave inclination θ_0 for different values of M_0/M_{CJ}. Again, heat release makes itself felt most significantly at the sonic point. In Figure 8(c), the maximum of $(a^2 + b^2)^{1/2}$ is plotted as a function of α for various Mach numbers. Unlike the corresponding graphs of Figures 6(c) and 7(c), the variation with Mach number is minimal here.

EFFECT OF DISTURBANCE ON DETONATION

Let us now examine the alteration in the structure of the detonation front caused by the passage of the disturbance. This will be done in the asymptotic limit of large activation energy. First, it is useful to recall the structure of the undisturbed oblique detonation, displayed schematically in Fig. 9. The structure consists of a lead shock S, across which the state of the mixture suffers a jump but the mass fraction retains the upstream value of unity since the shock is inert. Behind the shock lies the induction zone I in which the reaction is weak, and therefore, the state is undisturbed to leading order. The induction zone terminates in the fire zone F, which is a thin region of intense reaction. Behind the fire zone the mixture is fully burnt. The broadest feature of the detonation structure is the induction zone, whose thickness L_I effectively determines the detonation thickness. On the L_I scale, the shock is a discontinuity of course, but so is the fire zone in the limit $E \to \infty$. It can be shown that L_I has the asymptotic form

$$L_I = \frac{\overline{c}\hat{T}_0^2}{AE} e^{E/\hat{T}_0}, \tag{26}$$

where $\hat{T}_0$ is the undisturbed temperature immediately behind the lead shock. In the large E limit, it is possible to give an analytical treatment of the induction zone, in which state variables change by $O(E^{-1})$ and the position of the fire zone is characterized by a singularity in the induction-zone solution; the so-called thermal runaway. We now show that the primary effect of the applied disturbance is to produce relatively large ripples in the position of the fire zone.

In the induction zone, it is convenient to adopt the coordinate system $(\hat{\xi}, \hat{\eta})$, aligned with the undisturbed flow immediately behind the lead shock (Fig. 9). The dependent variables are denoted by hatted quantities as well, and the subscript zero corresponds to undisturbed flow. Also, the induction-zone thickness L_I is chosen as the reference length. Then, equations (1a-f) apply again, provided all variables are hatted. Also, the reaction rate Λ now has the form

$$\Lambda = \frac{AL_I}{\overline{c}} \hat{Y} e^{-E/\hat{T}},$$

which, in view of (26), can be expresed as

$$\Lambda = \frac{\hat{T}_0^2}{E} \hat{Y} exp\left[\frac{E}{\hat{T}_0} - \frac{E}{\hat{T}}\right]. \tag{27}$$

As before, the state of the gas behind the lead shock can be computed by means of the jump conditions (2), provided α is set to zero there.

Although we have chosen to refer all lengths to L_I in the induction zone, it must be recognized that along the shock, i.e., in the y-direction, the proper length scale is still L_0. Therefore, on the L_I scale, y-derivatives must be of order L_I/L_0, and hence negligible to an excellent approximation. Thus, for any dependent variable F,

$$F_y = F_{\hat{\xi}} \sin\hat{\varphi}_0 + F_{\hat{\eta}} \cos\hat{\varphi}_0 = O(L_I/L_0) \ll 1,$$

whence

$$F_{\hat{\eta}} \sim -\tan\hat{\varphi}_0 F_{\hat{\xi}}.$$

The governing equations are thus rendered quasi-one-dimensional in the induction zone.

Let us now consider a distinguished limit in which the applied disturbance amplitude is $\hat{T}_0^2/E$. Then, for $E \to \infty$, the governing equations reduce to

$$\hat{u}_0\hat{\rho}'_{\hat{\xi}} + \hat{\rho}_0(\hat{u}'_{\hat{\xi}} - \tan\hat{\varphi}_0\hat{v}'_{\hat{\xi}}) = 0, \tag{28a}$$

$$\hat{\rho}_0\hat{u}_0\hat{u}'_{\hat{\xi}} + (1/\gamma)\hat{p}'_{\hat{\xi}} = 0, \tag{28b}$$

$$\hat{\rho}_0\hat{u}_0\hat{v}'_{\hat{\xi}} - (1/\gamma)\tan\hat{\varphi}_0\hat{p}'_{\hat{\xi}} = 0, \tag{28c}$$

$$\hat{\rho}_0\hat{u}_0\hat{T}'_{\hat{\xi}} - \frac{\gamma-1}{\gamma}\hat{u}_0\hat{p}'_{\hat{\xi}} = \alpha e^{\hat{T}'}, \tag{28d}$$

$$\hat{p}' = \hat{\rho}_0\hat{T}' + \hat{T}_0\hat{\rho}'. \tag{28e}$$

In the above equations, primes denote perturbations. It is a simple matter to extract from these equations, by elimination, a single equation for the temperature perturbation $\hat{T}'$, i.e.,

$$\hat{T}'_{\hat{\xi}} = \Gamma e^{\hat{T}'}, \tag{29}$$

where

$$\Gamma = \left(\frac{\alpha\gamma}{\hat{u}_0\hat{\rho}_0}\right)\frac{(1/\gamma) - \hat{\mu}_n^2}{1-\hat{\mu}_n^2}, \tag{30}$$

and $\hat{\mu}_n$ is the normal Mach number of the undisturbed flow immediately behind the shock. We remark parenthetically that for Γ to be positive, $\hat{\mu}_n < 1/\sqrt{\gamma}$, i.e., the normal flow speed immediately behind the shock must be less than the isothermal sound speed, a well-known restriction (see, for example, Clarke [6]). It is now a simple matter to integrate equation

(29) provided $\hat{T}'_s(\hat{\eta})$, the value of the temperature perturbation at the shock, is known. Then, one obtains

$$\hat{T}' = -\ln\left[e^{-\hat{T}'_s} - \Gamma\hat{\xi}\right]. \tag{31}$$

The actual profile of $\hat{T}'$ is of less interest than the position at which it becomes singular. This position is given by

$$\hat{\xi}_f = (1/\Gamma)e^{-\hat{T}'_s}, \tag{32}$$

and defines the location of the fire zone. For the undisturbed detonation, $\hat{T}'_s = 0$ and the fire-zone location is given by $\hat{\xi}_{f0} = 1/\Gamma$. The shift in location is therefore $\hat{\xi}_f - 1/\Gamma$. Note that the shift is an O(1) quantitity, on the scale of the induction length, while the disturbance amplitude causing the shift is $O(E^{-1})$. The applied disturbance, therefore, has a pronounced effect on the internal structure of the detonation wave. This is illustrated in Figure 10 for a sinusoidal temperature perturbation at the shock. Once $\hat{T}'$ is known, equations (28a-e) can be integrated, subject to appropriate conditions at the shock, thus yielding the profiles for all the variables in the induction zone.

CONCLUSIONS

On the whole, then, the effect of exothermicity is to amplify the refracted waves. This result, although derived here only for steady waves, contradicts that of Kumar, Bushnell and Hussaini [7]. However, they simulated numerically the interaction of a disturbance with an oblique shock with *equilibrium chemistry*, and found that chemistry led to a slight decrease in amplification. We believe that their result is biased by the manner in which they prespecify the degree of reactedness at each station. It would be more appropriate to compare our results with a direct numerical simulation of the reacting shock, undertaken, for example, by extending the approach of Zang, Hussaini and Bushnell [4] to reactive flows.

APPENDIX

In this Appendix are listed the various constants introduced in the text.

$$A = \sec\varphi_0 + 2(r-1)\cos\varphi_0 + (a/r)(r-1)^2\sin\varphi_0,$$

$$B = (b/r)(r-1)^2\sin\varphi_0,$$

$$a = \begin{cases} r\frac{CE+DF}{C^2+D^2} & \text{for } \mu < 1, \\ r\frac{C'+GF'}{E'+GD'} & \text{for } \mu > 1, \end{cases}$$

$$b = r\frac{CF-DE}{C^2+D^2},$$

$$C = [d + 2r - 1 - (r-1)/\beta_n^2]\tan\varphi_0 - [(r-1)^2/\beta_n^2]\sin\varphi_0\cos\varphi_0,$$

$$C' = 1 - d - 2[1 + (r-1)\cos^2\varphi_0],$$

$$D = \beta D'/\beta_n^2,$$

$$D' = (r-1)[1 + (r-1)\cos^2\varphi_0],$$

$$E = 1 + d + 2(r-1)(\beta^2/\beta_n^2)\cos^2\varphi_0,$$

$$E' = (r-1)^2\sin\varphi_0\cos\varphi_0 - (d+r)\tan\varphi_0,$$

$$F = (\beta/\beta_n^2)F',$$

$$F' = 2(r-1)\sin\varphi_0\cos\varphi_0,$$

$$G = \frac{1 - \beta \tan \varphi_0}{\beta + \tan \varphi_0},$$

$$C_1 = ar^{-1}D' - F',$$

$$C_2 = br^{-1}D'.$$

REFERENCES

1. Ribner, H. S., "Convection of a pattern of vorticity through a shock wave", NACA Report 1164 (1954).

2. McKenzie, J. F. and Westphal, K. O., "Interaction of linear waves with obligue shock waves", Physics of Fluids, 11, pp. 2350-2362 (1968).

3. O'Brien, C. J. and Kobayashi, A. C., "Advanced earth-to- orbit propulsion concepts", AIAA/SAE/ASME/ASEE 23rd Joint Propulsion Conference. AIAA-86-1386, Huntsville, Alabama, June 1986.

4. Zang, T. A., Hussaini, M. Y. and Bushnell, D. M., "Numerical computations of turbulence amplification in shock-wave interactions", AIAA J., 22, pp. 13-21(1984).

5. Anyiwo, J. C. and Bushnell, D. M., "Turbulence amplification in shock-wave boundary layer interaction", AIAA J., 20, pp. 893-899 (1982).

6. Clarke, J. F., "Combustion and compressibility in gases", Mathematical Modeling in Combustion and Related Topics, C. M. Brauner and C. Schmidt-Laine (eds.), pp. 43-63 1988), Martinus Nijhoff Publishers.

7. Kumar, A., Bushnell, D. M. and Hussaini, M. Y., "A mixing augmentation technique for hypervelocity scramjets", In AIAA/SAE/ASME/ASEE 23rd Joint Propulsion Conference, AIAA-87-1882, San Diego, June 1987.

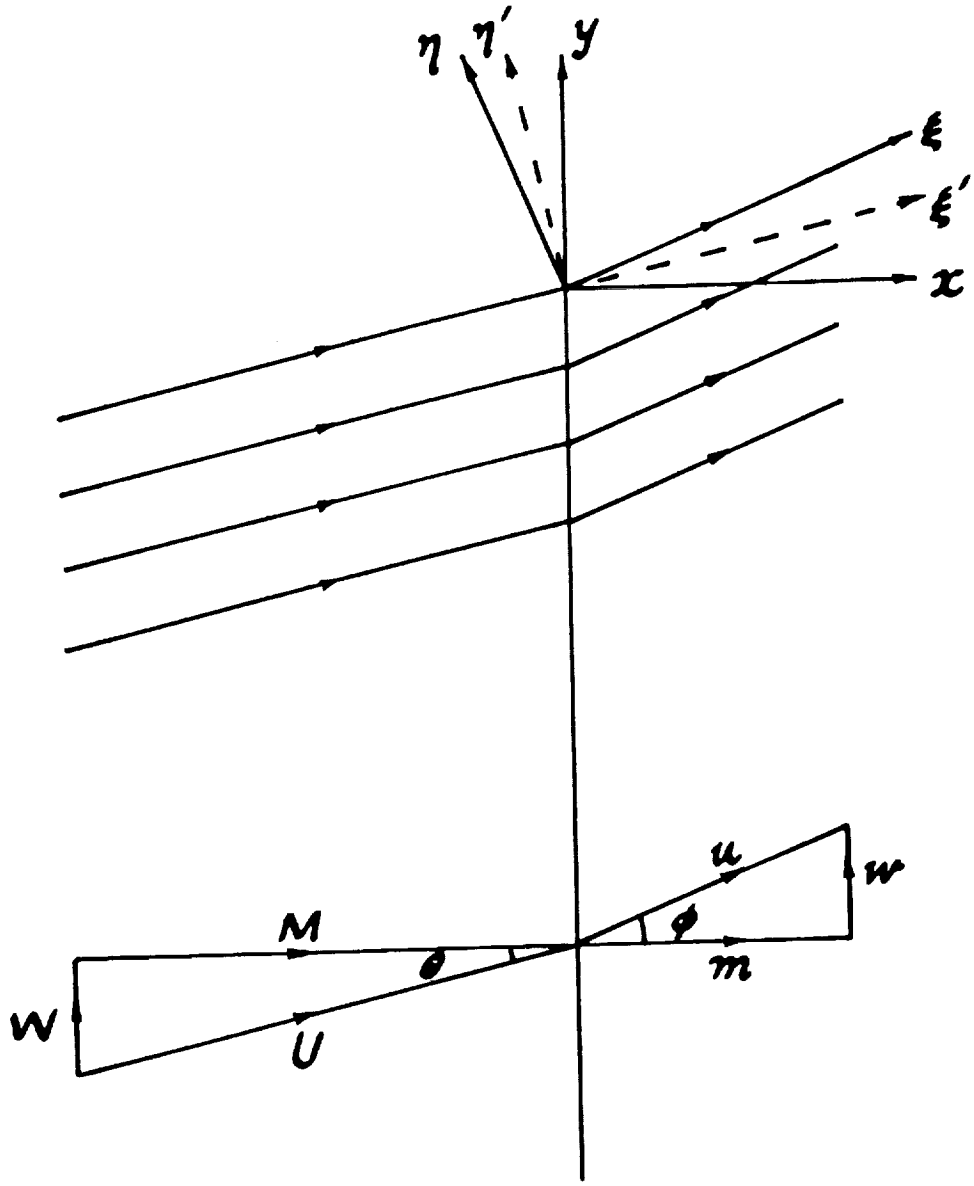

Figure 1. Illustration of a stationary, planar, oblique detonation wave and the coordinate frame.

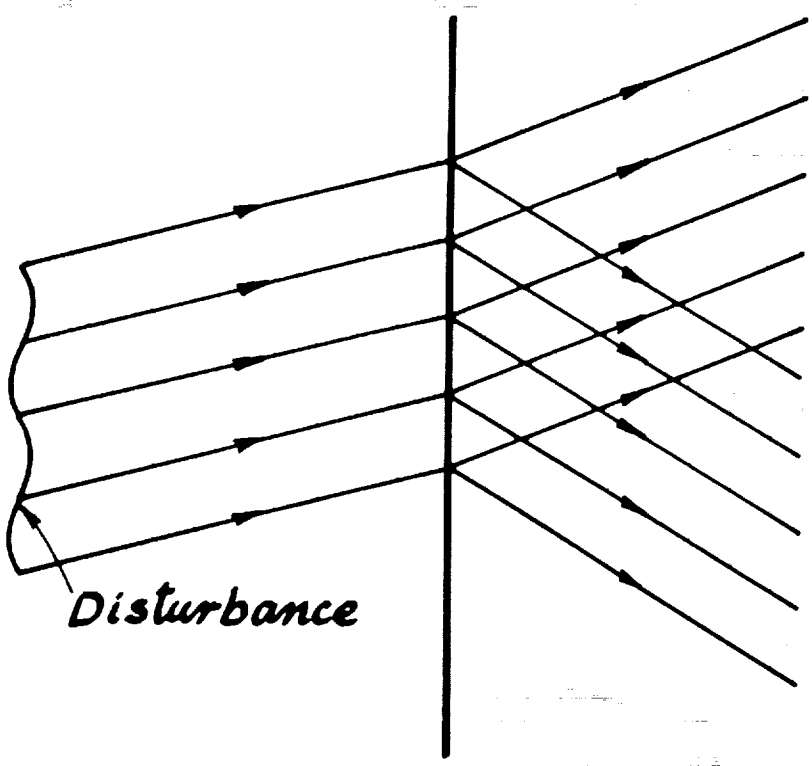

Figure 2. Schematic of a planar, steady, shear disturbance superimposed on the incident stream.

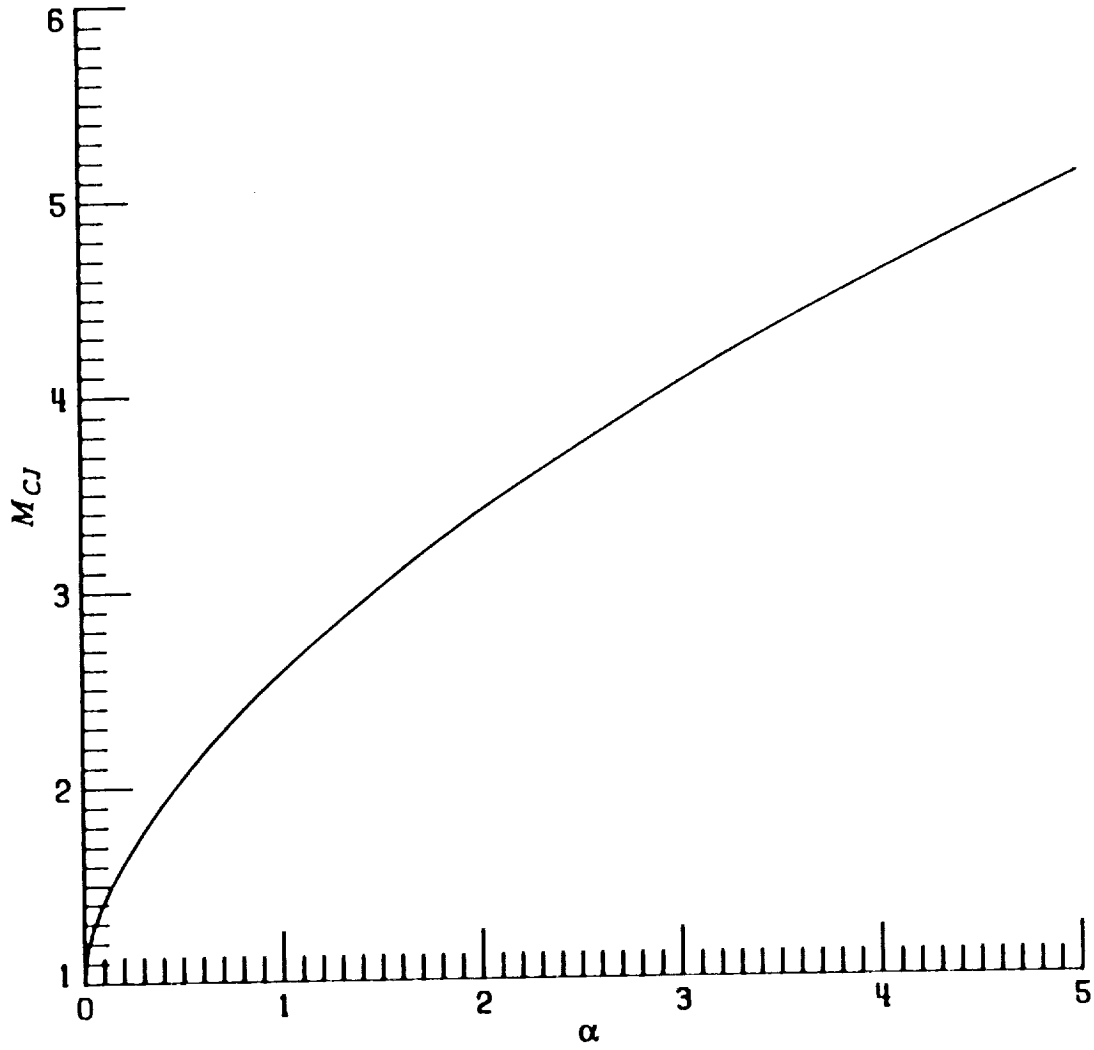

Figure 3. Plot of the Chapman-Jouguet Mach number M_{CJ} versus the heat release parameter α.

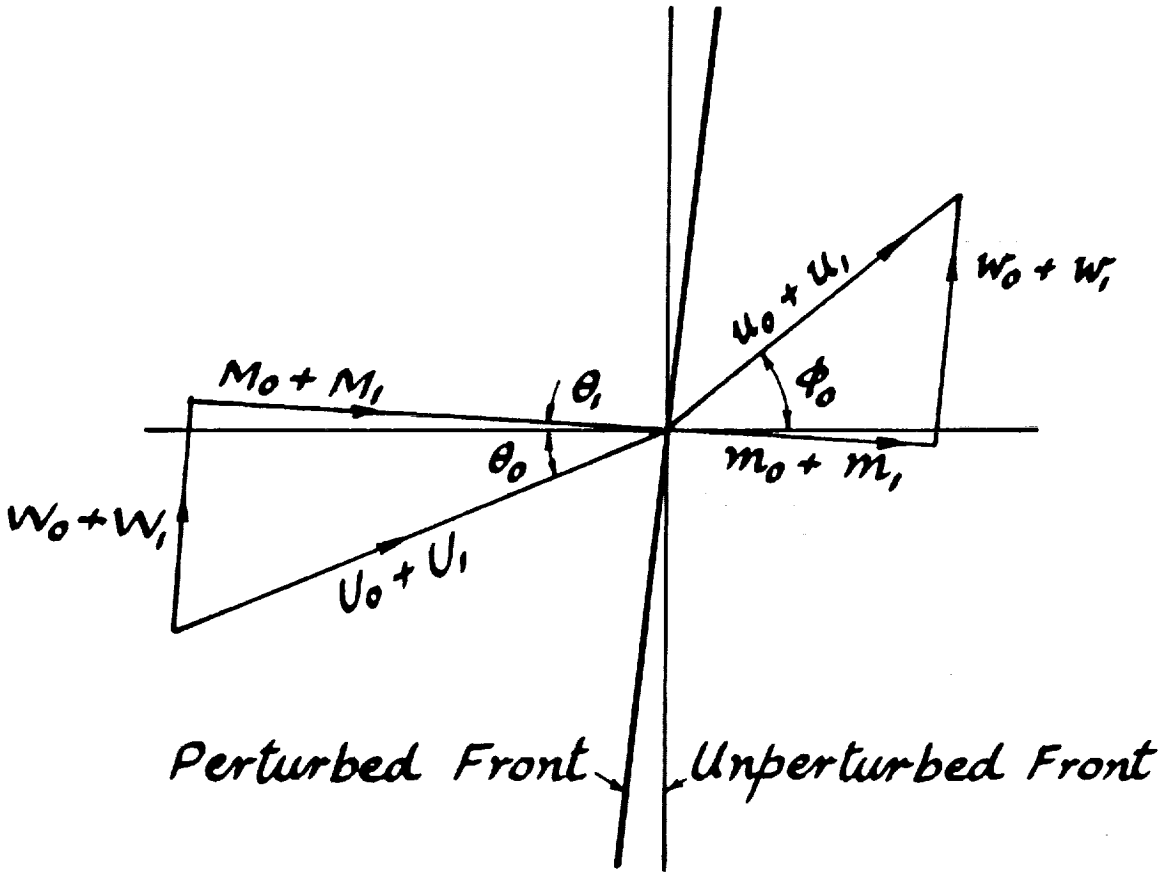

Figure 4. Schematic of the perturbed upstream flow showing the nomenclature.

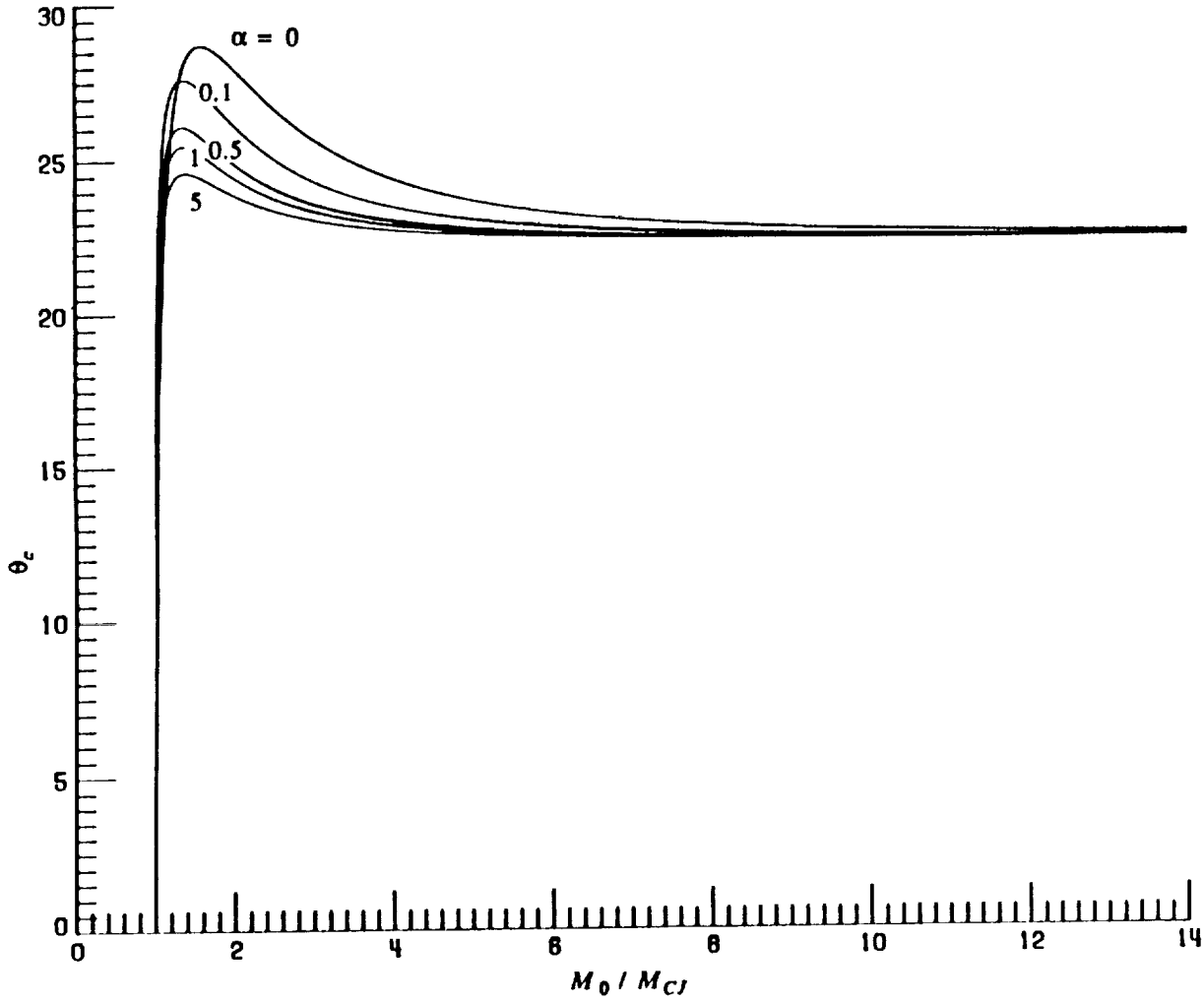

Figure 5. Plot of the critical angle θ_c versus the upstream normal Mach number M_0 / M_{CJ} for α = 0, 0.1, 0.5, 1, 5.

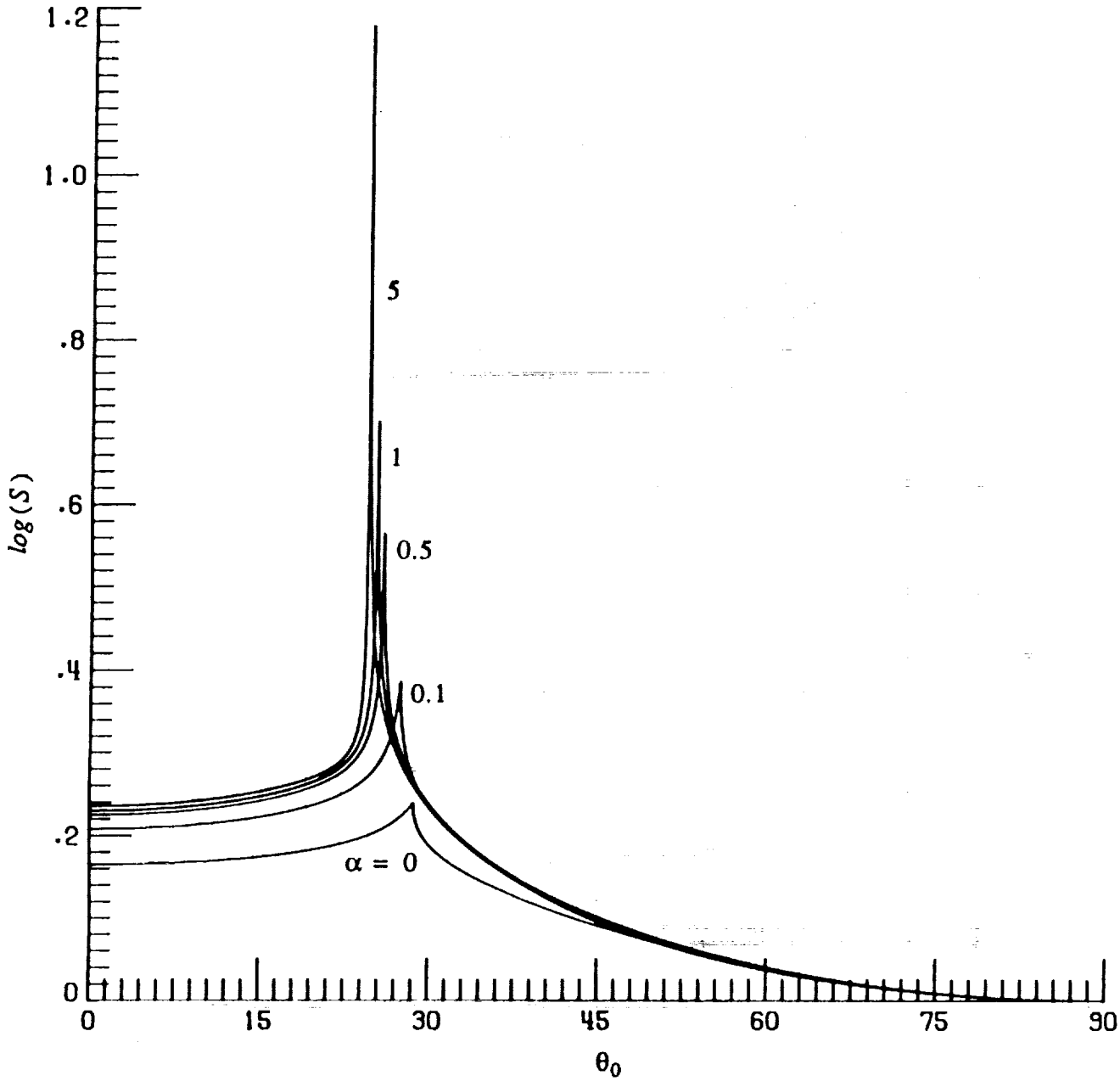

Figure 6a. Plot of the amplitude log(S) versus the wave inclination angle θ_0, at $M_0 / M_{CJ} = 1.5$, for $\alpha = 0, 0.1, 0.5, 1, 5$.

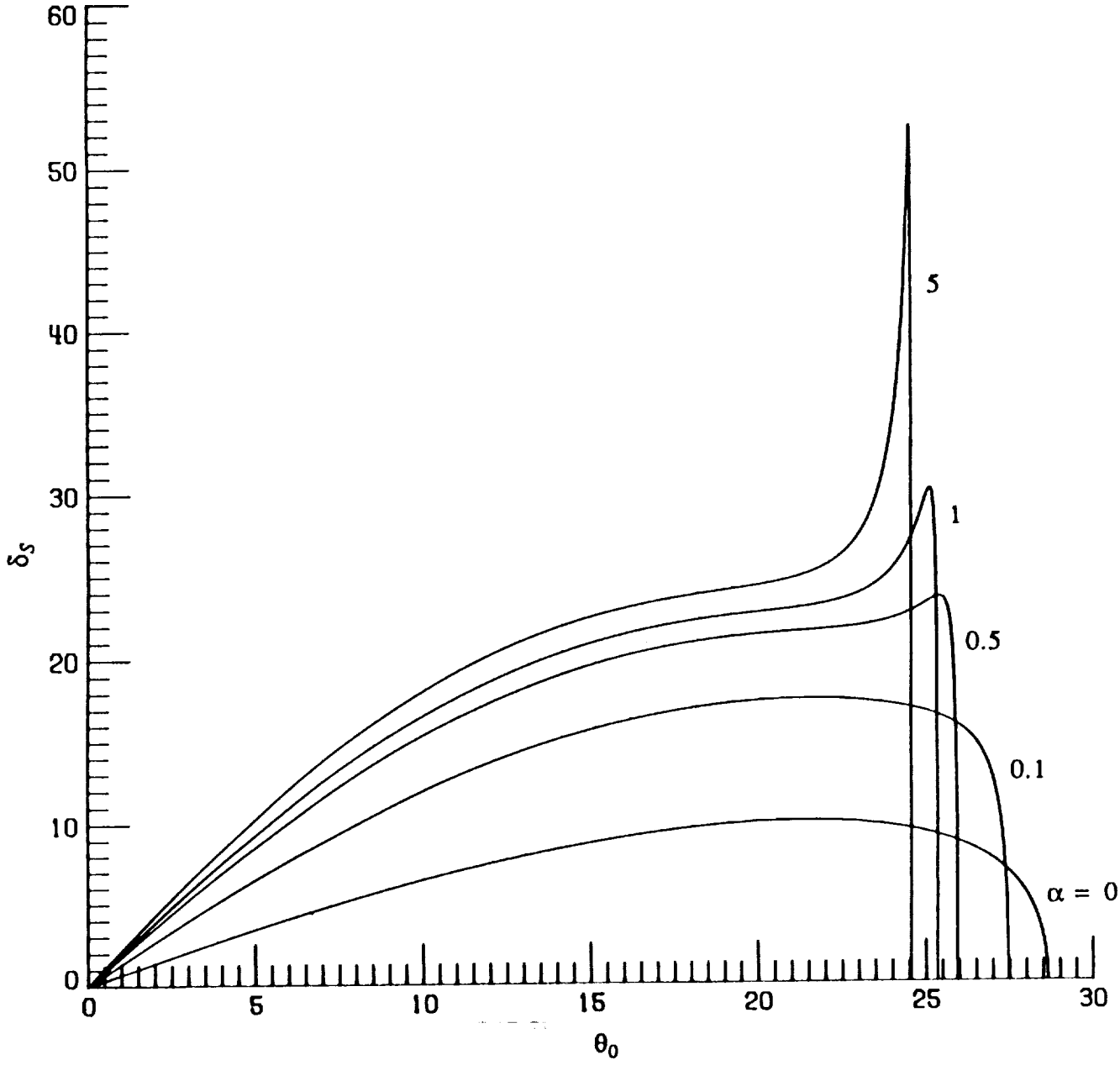

Figure 6b. Plot of the phase shift δ_s versus the wave inclination angle θ_0, at $M_0 / M_{CJ} = 1.5$, for $\alpha = 0, 0.1, 0.5, 1, 5$.

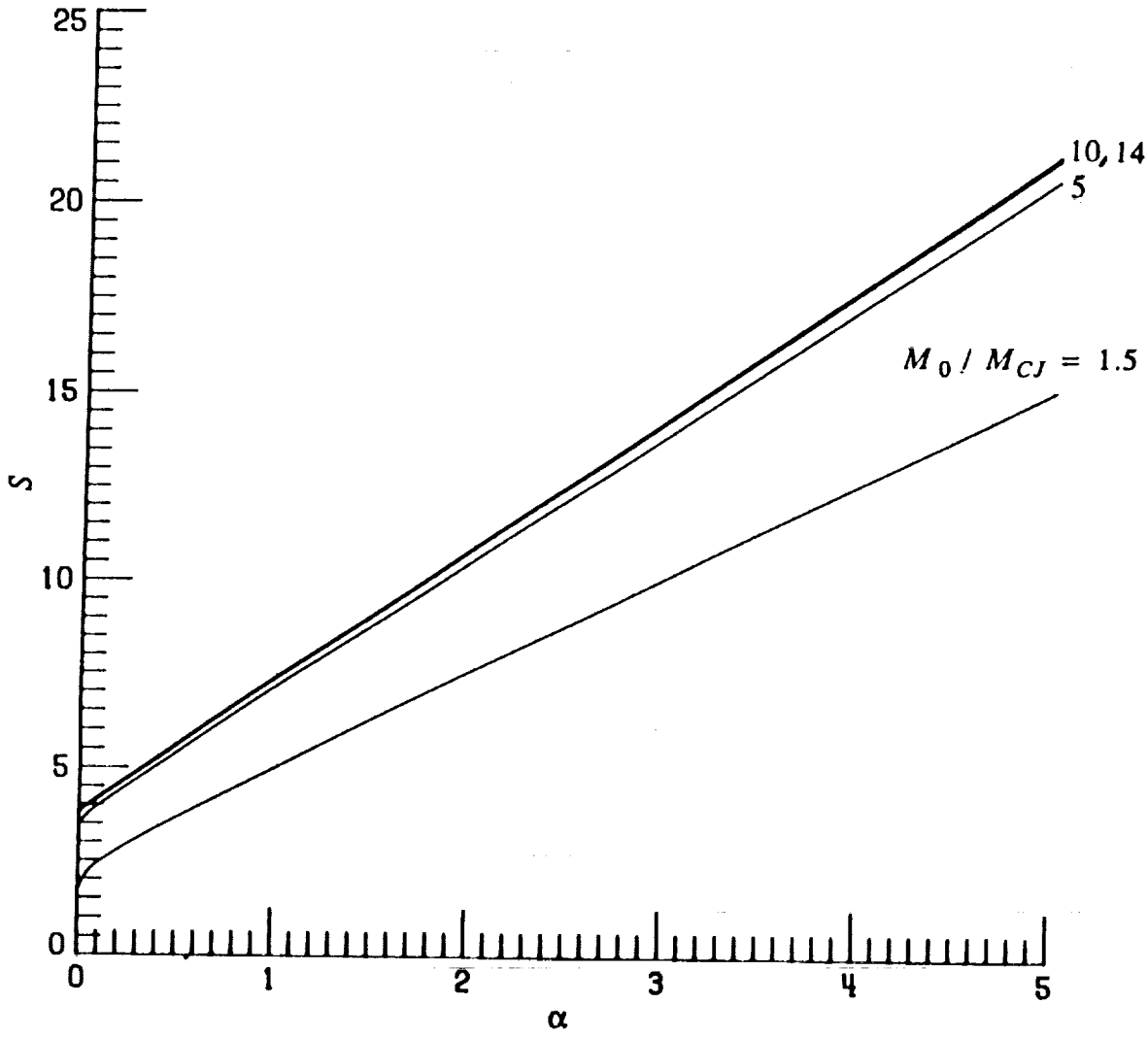

Figure 6c. Plot of the maximum amplitude of S versus the heat release parameter α, for M_0 / M_{CJ} = 1.5, 5, 10, 14, at θ_c.

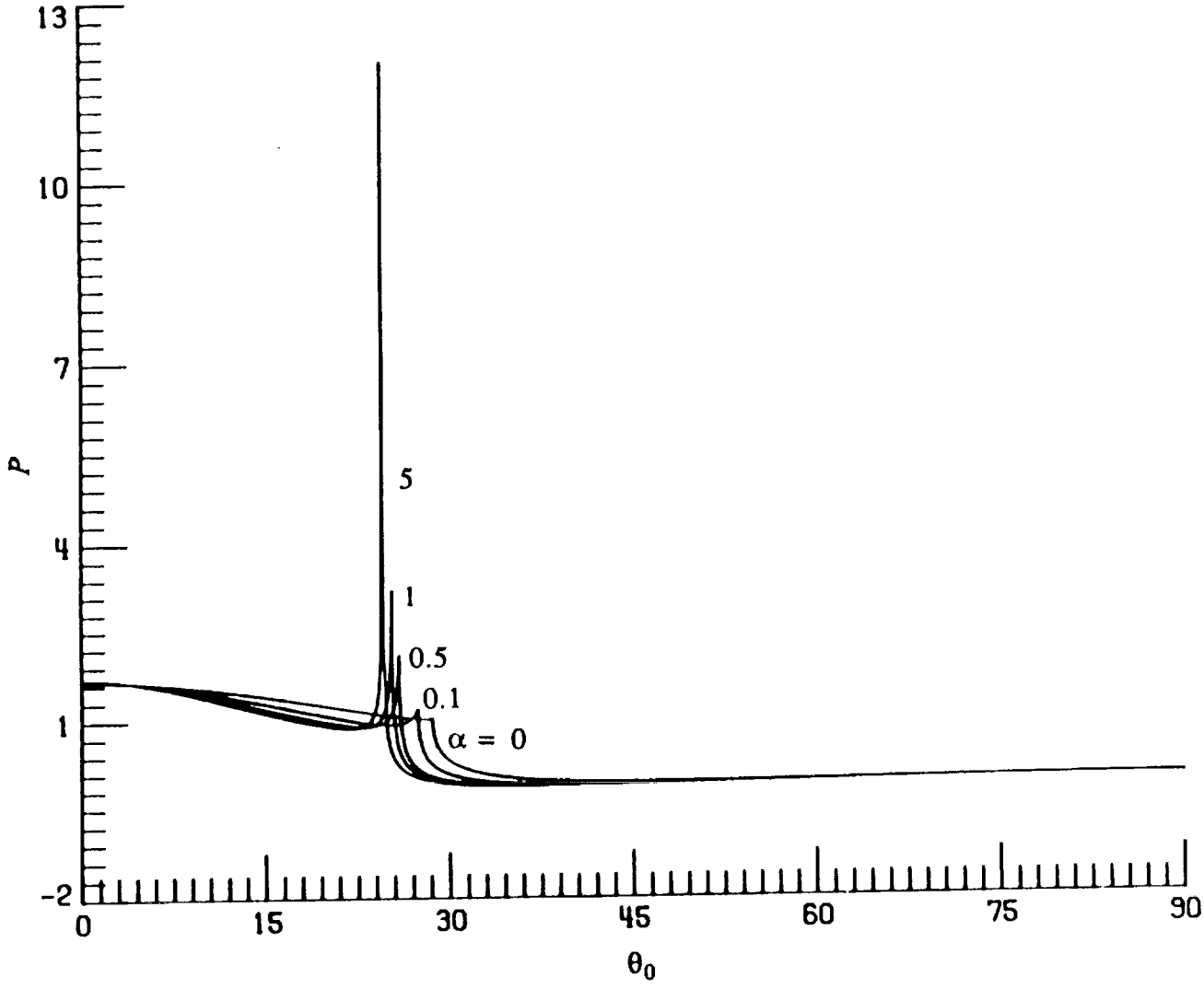

Figure 7a. Plot of the amplitude P versus the wave inclination angle θ_0, at $M_0 / M_{CJ} = 1.5$, for $\alpha = 0, 0.1, 0.5, 1, 5$.

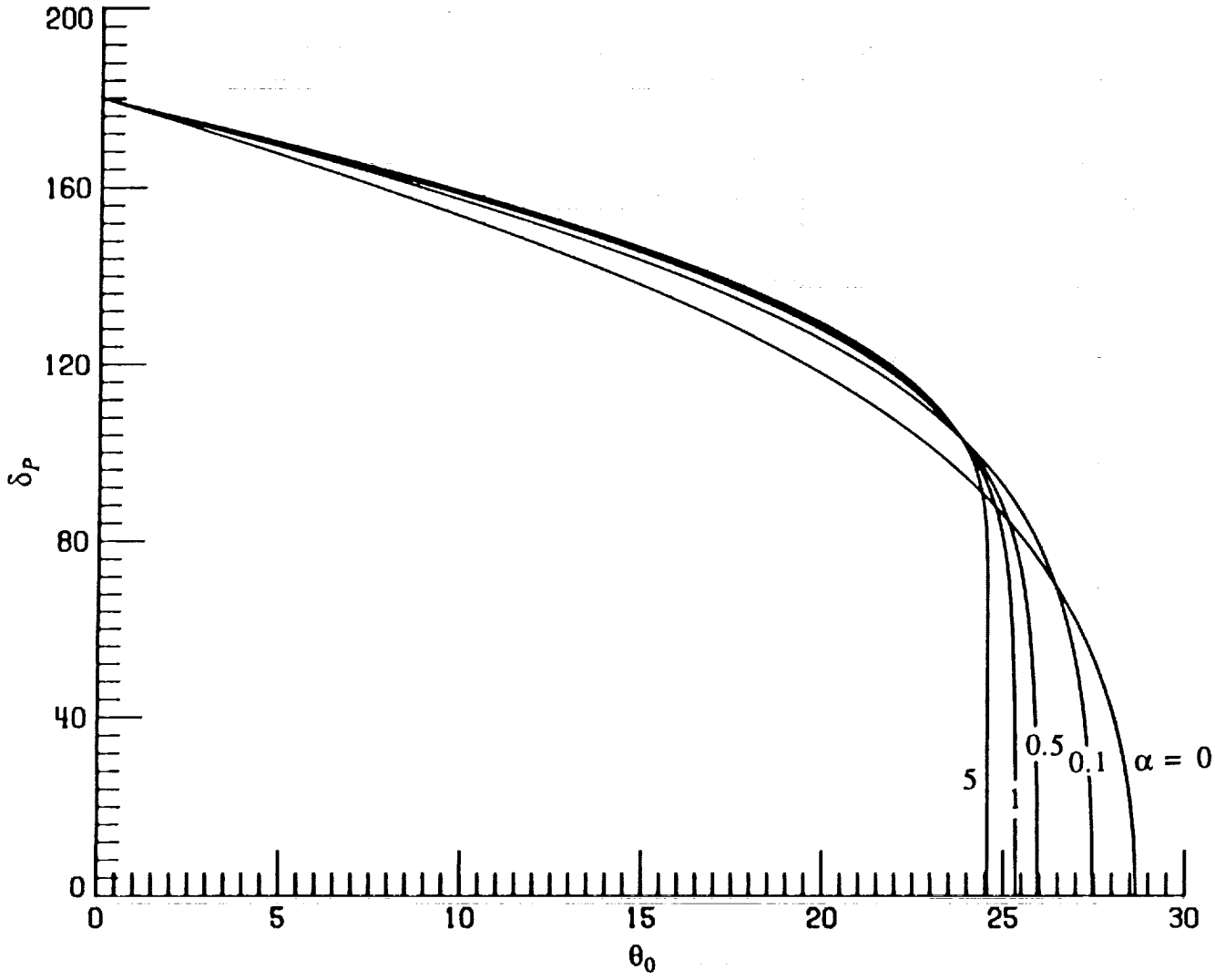

Figure 7b. Plot of the phase shift δ_P versus the wave inclination angle θ_0, at $M_0 / M_{CJ} = 1.5$, for $\alpha = 0, 0.1, 0.5, 1, 5$.

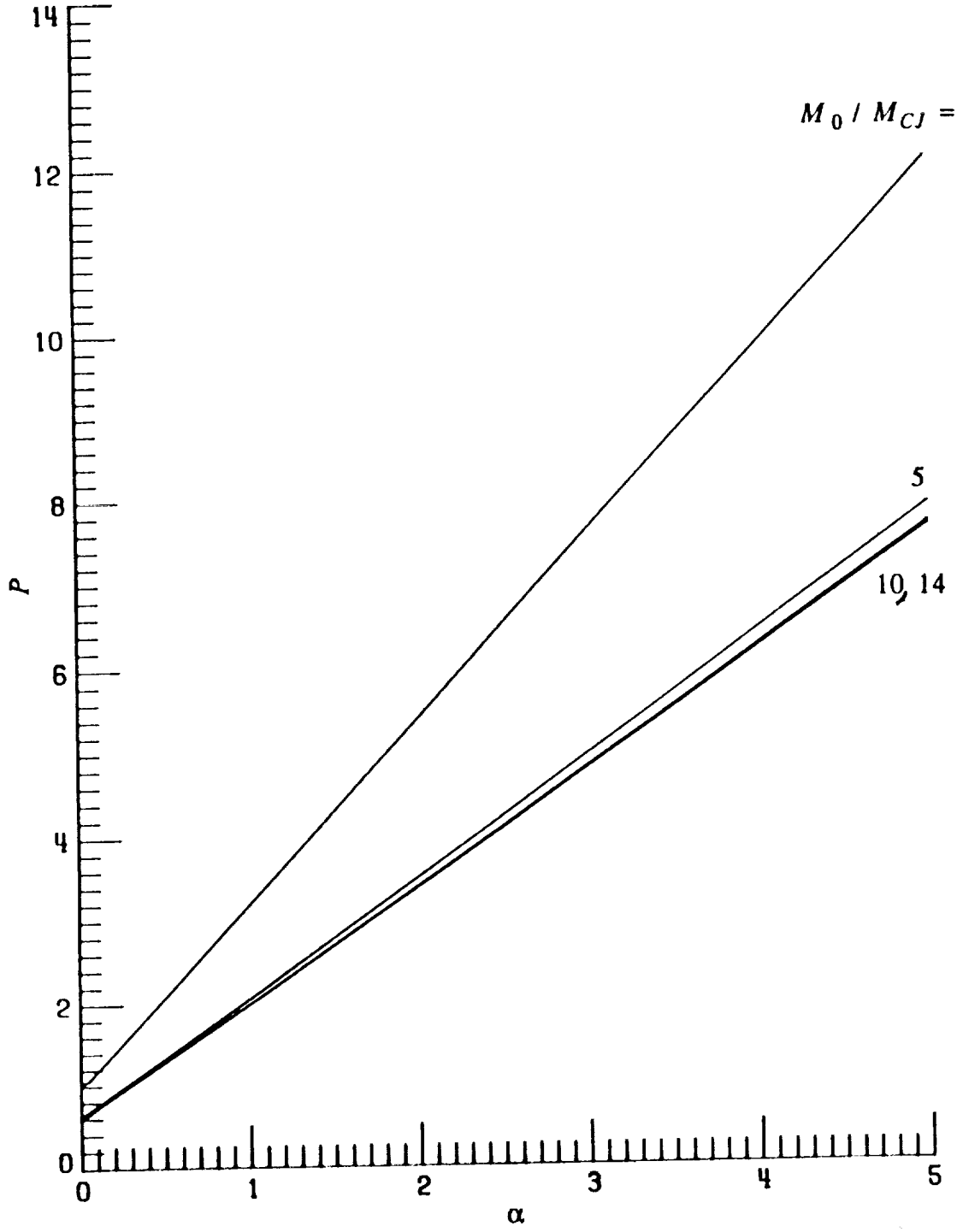

Figure 7c. Plot of the maximum amplitude of P versus the heat release parameter α, for M_0 / M_{CJ} = 1.5, 5, 10, 14, at θ_c.

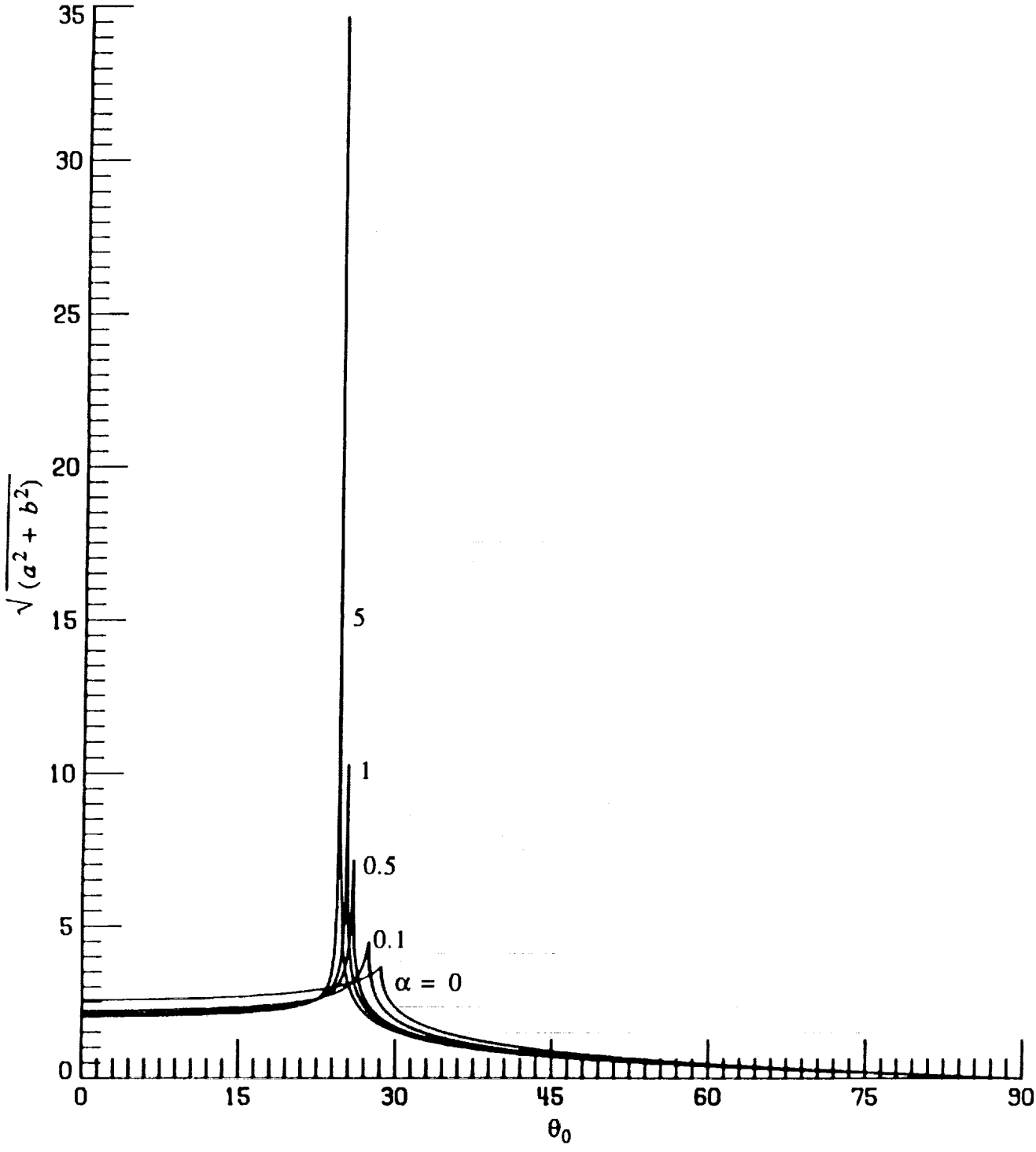

Figure 8a. Plot of $\sqrt{(a^2 + b^2)}$ versus the wave inclination angle θ_0, at $M_0 / M_{CJ} = 1.5$, for $\alpha = 0, 0.1, 0.5, 1, 5$.

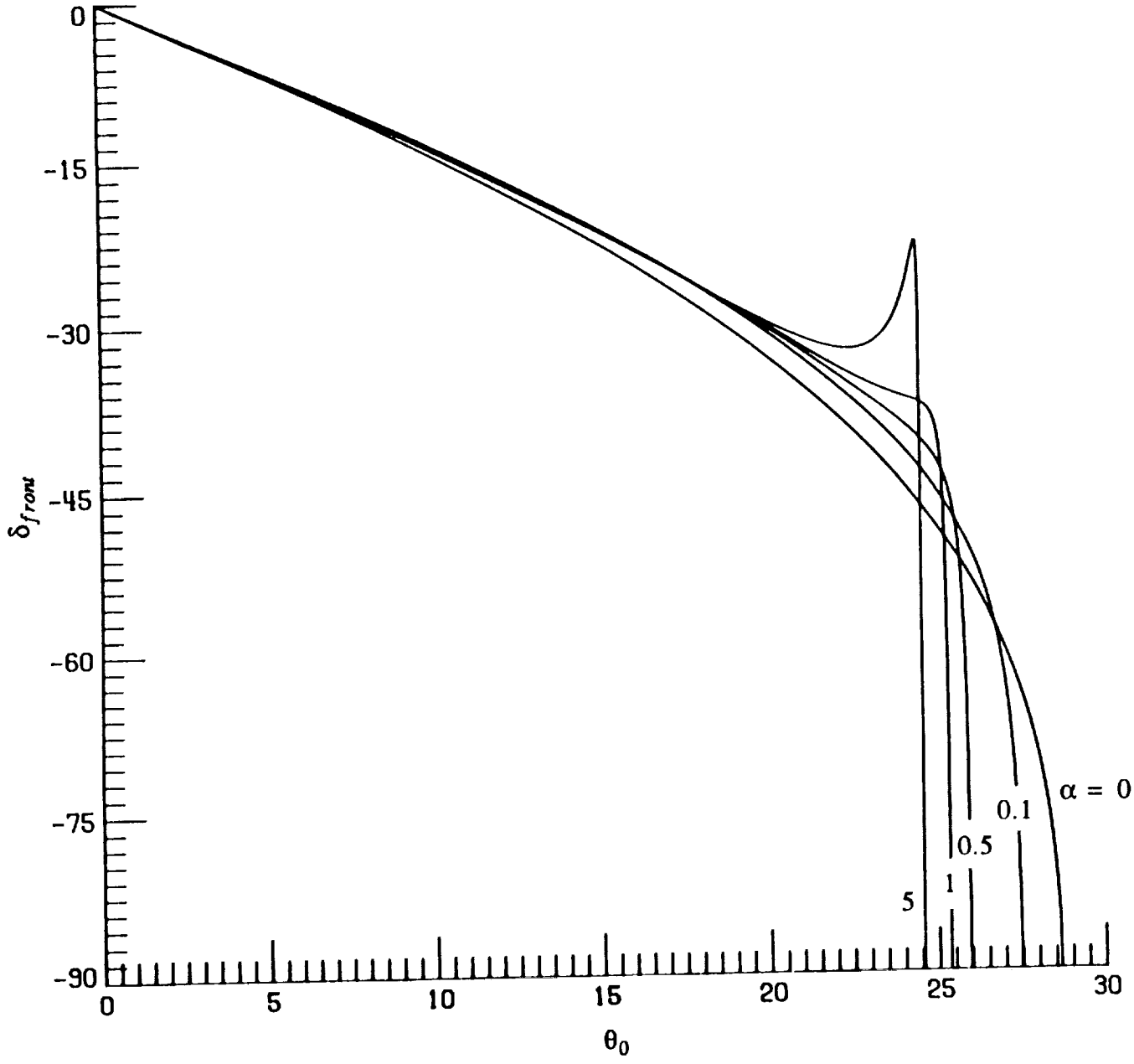

Figure 8b. Plot of δ_{front} versus the wave inclination angle θ_0, at $M_0 / M_{CJ} = 1.5$, for $\alpha = 0, 0.1, 0.5, 1, 5$.

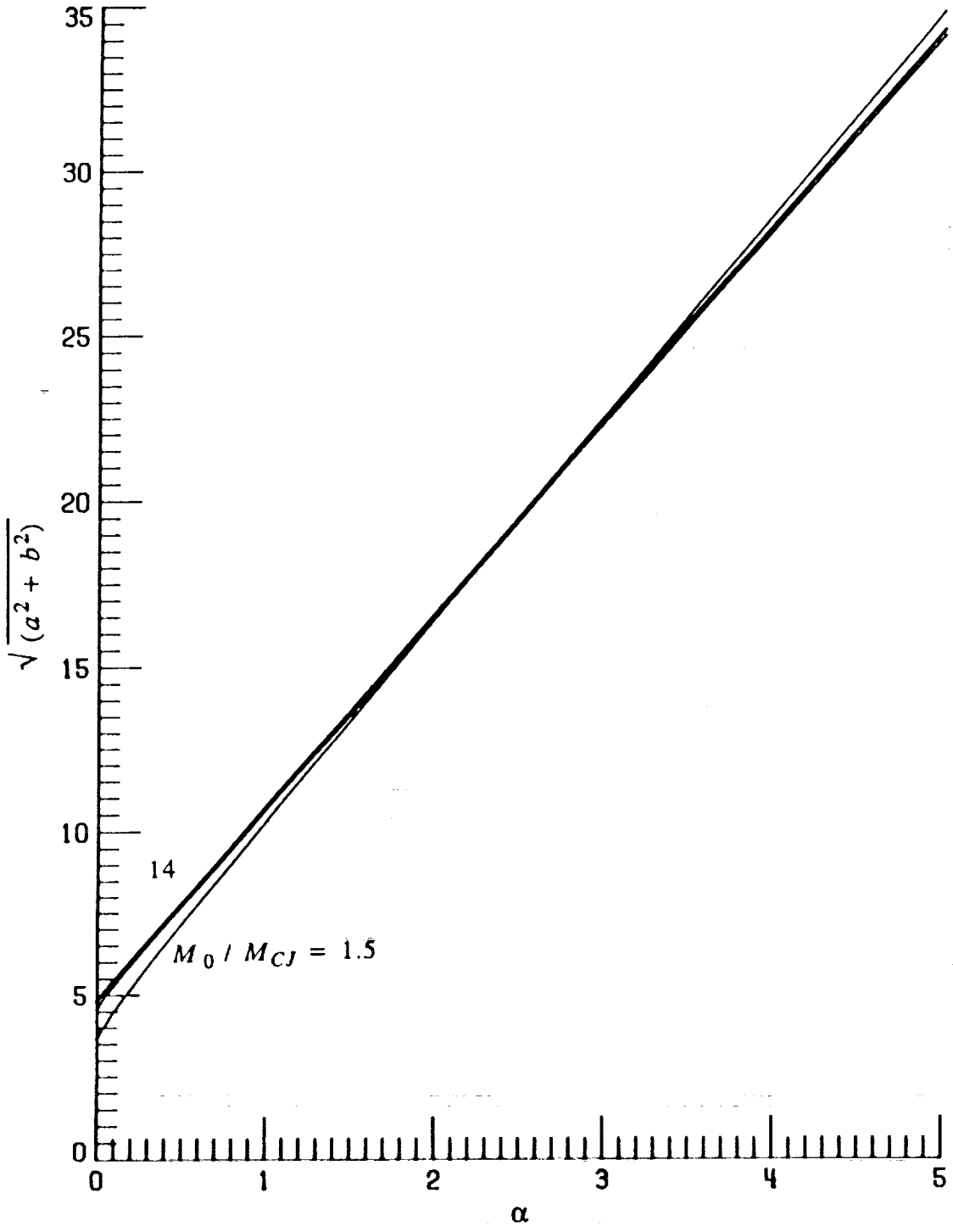

Figure 8c. Plot of the maximum of $\sqrt{(a^2 + b^2)}$ versus the heat release parameter α, for M_0 / M_{CJ} = 1.5, 5, 10, 14, at θ_c. (Graphs for M_0 / M_{CJ} of 5, 10, and 15 are indistinguishable).

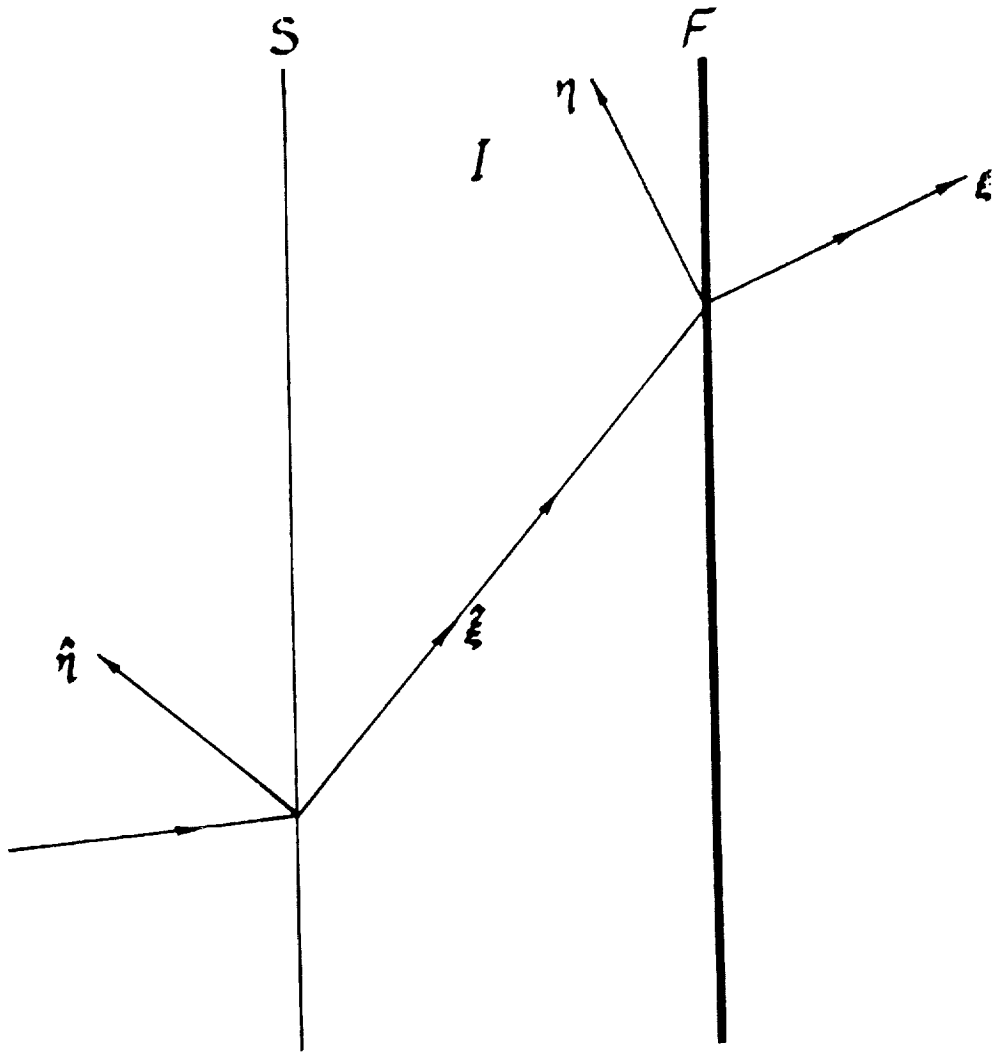

Figure 9. Schematic of the coordinate system aligned with the undisturbed flow immediately behind the lead shock.

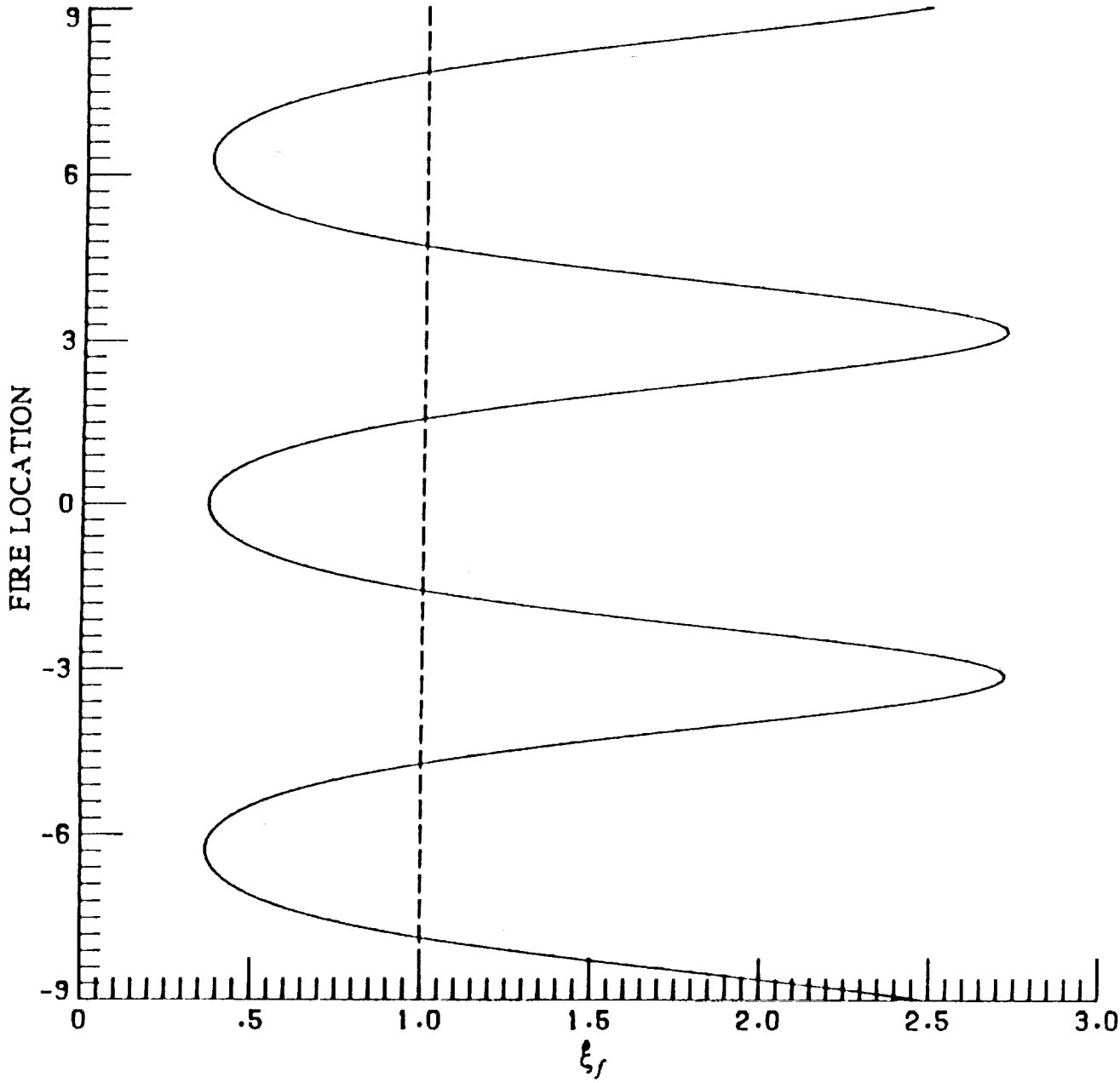

Figure 10. Plot of the unperturbed (dashed) and perturbed (solid) fire-zone location for a sinusoidal temperature perturbation at the shock.

NASA
National Aeronautics and Space Administration

Report Documentation Page

1. Report No.	2. Government Accession No.	3. Recipient's Catalog No.
NASA CR-181921 ICASE Report No. 89-68		

4. Title and Subtitle

CONVECTION OF A PATTERN OF VORTICITY THROUGH A REACTING SHOCK WAVE

5. Report Date

September 1989

6. Performing Organization Code

7. Author(s)

T. L. Jackson
A. K. Kapila
M. Y. Hussaini

8. Performing Organization Report No.

89-68

10. Work Unit No.

505-90-21-01

9. Performing Organization Name and Address

Institute for Computer Applications in Science and Engineering
Mail Stop 132C, NASA Langley Research Center
Hampton, VA 23665-5225

11. Contract or Grant No.

NAS1-18107
NAS1-18605

12. Sponsoring Agency Name and Address

National Aeronautics and Space Administration
Langley Research Center
Hampton, VA 23665-5225

13. Type of Report and Period Covered

Contractor Report

14. Sponsoring Agency Code

15. Supplementary Notes

Langley Technical Monitor:
Richard W. Barnwell

Physics of Fluids, Series A

Final Report

16. Abstract

The passage of a weak vorticity disturbance through a reactive shock wave, or detonation, is examined by means of a linearized treatment. Of special interest is the effect of chemical heat release on the amplification of vorticity in particular, and on the disturbance pattern generated downstream of the detonation in general. It is found that the effect of exothermicity is to amplify the refracted waves. The manner in which the imposed disturbance alters the structure of the detonation itself is also discussed.

17. Key Words (Suggested by Author(s))	18. Distribution Statement
detonation, vorticity, heat release	59 - Mathematical and Computer Sciences 34 - Fluid Mechanics and Heat Transfer Unclassified - Unlimited

19. Security Classif. (of this report)	20. Security Classif. (of this page)	21. No. of pages	22. Price
Unclassified	Unclassified	31	A03

NASA FORM 1626 OCT 86